Journal of Thermal Analysis, Vol. 53 (1998) 111-121

# THERMOGRAVIMETRIC ANALYSIS OF VANADIUM PHOSPHORUS OXIDE CATALYSTS DOPED WITH COBALT AND IRON

*V. Martin, J. M. M. Millet and J. C. Volta*

Institut de Recherches sur la Catalyse, CNRS, conventionné avec l'Université Claude Bernard Lyon I, 2 avenue A. Einstein, F-69626 Villeurbanne Cedex, France

(Received July 17, 1997)

## Abstract

The transformation of $VOHPO_4 \cdot 0.5H_2O$ (VPO) precursor doped with cobalt or iron for *n*-butane oxidation to maleic anhydride was investigated by thermogravimetric analysis under air and nitrogen, with and without *n*-butane in the flow. While almost no effect was observed in nitrogen or air, a strong influence of the doping was observed when *n*-butane was added to the nitrogen or air. This resulted in a delay of the decomposition of the precursor and a further reoxidation of the VPO catalyst, particularly for doping with cobalt at low percentage (1%). This shows that doping can change the oxidation state of vanadium phosphorus oxide catalysts, which can explain differences in their catalytic performances and the favourable effect of doping by cobalt.

**Keywords:** air, cobalt dopant, iron dopant, *n*-butane, nitrogen, thermogravimetric analysis, vanadium phosphorus oxides

## Introduction

Vanadium phosphorus oxide (VPO) is known as the most efficient catalyst for *n*-butane oxidation to maleic anhydride [1–5]. This catalyst is prepared from a precursor, $VOHPO_4 \cdot 0.5H_2O$ ($V^{4+}$) [6], which can be activated under nitrogen or directly under an *n*-butane/air atmosphere (1–3% vol.) to give the vanadyl pyrophosphate $(VO)_2P_2O_7$ ($V^{4+}$) phase, which is the effective catalyst evidenced by X-ray diffraction. The oxidation state measured for vanadium in the equilibrated VPO catalyst is close to 4, in agreement with the main contribution of the $(VO)_2P_2O_7$ phase, but it can be slightly higher, particularly at the beginning of the activation. The superficial relative amounts of $V^{4+}$ and $V^{5+}$ can be measured by XPS from the decomposition of the $V_{2p}^{3/2}$ XPS peaks observed at 516.9 and 518.0 eV, respectively [7], while the relative distribution of $VOPO_4$ structures ($V^{5+}$) *vs.* $(VO)_2P_2O_7$ ($V^{4+}$) can be estimated by $^{31}P$ NMR (MAS and spin echo

1418–2874/98/ $ 5.00

Akadémiai Kiadó, Budapest
Kluwer Academic Publishers, Dordrecht

mapping) [7, 8]. By combining these techniques, a scheme for the activation of the $VOHPO_4 \cdot 0.5H_2O$ precursor under an *n*-butane/air atmosphere was proposed. This transformation follows two independent and parallel routes of dehydration to $(VO)_2P_2O_7$ ($V^{4+}$) and concerted dehydration and oxidation to transient $VOPO_4$ phases ($V^{5+}$) [7]. It has been demonstrated by *in situ* Raman spectroscopy that the incorporation of dopants such as Co or Fe can change the $V^{5+}/V^{4+}$ balance during the activation period and can therefore change the catalytic performances in the stationary state for *n*-butane oxidation to maleic anhydride [9]. In this work we study the effects of cobalt and iron added as dopants to the VPO precursor on the thermal behavior, depending on the atmosphere considered.

## Experimental

### *Preparation of undoped and doped $VOHPO_4 \cdot 0.5H_2O$ precursors*

These preparations have already been described [9]. Undoped precursor $VOHPO_4 \cdot 0.5H_2O$ was prepared by adding $V_2O_5$ (11.8 g) to isobutanol (250 ml). $H_3PO_4$ (16.49 g, 85%) was then introduced to the mixture, which was refluxed for 16 h. The light-blue suspension was next separated from the organic solution by filtration, and washed with isobutanol (200 ml) and ethanol (150 ml, 100%). The resulting solid was refluxed in water (9 ml $H_2O$/g solid), filtered hot and dried in air (110°C, 16 h). For the preparation of the doped 1% Fe and Co/V and 5% Co/V precursors, the required mass of the corresponding acetylacetonate salts was previously dissolved in isobutanol according to the atomic stoichiometry, prior to the operation of refluxing with isobutanol and 85% $H_3PO_4$. Further operations of filtration and washing were carried out as for the undoped precursor. The four precursors were then dried at 120°C under air for 12 h.

The synthesized precursors, designated VPO, were chemically analyzed and their dopant to vanadium ratio, Co/V or Fe/V, was determined (Table 1). For example, this ratio is given as VPOCo1 for a precursor doped with 1% of cobalt cations.

### *Thermogravimetric analyses*

Thermogravimetric analyses were performed with a Setaram TGA-DTA 92 thermobalance. 30–34 mg of sample was placed in a platinum crucible suspended from one arm of the balance. The temperature was raised to 530°C at a heating rate of 1.25°C $min^{-1}$ and maintained at this temperature for 3 h. The analyses were conducted at atmospheric pressure under the same flow (2.4 l $h^{-1}$) of air, nitrogen or a mixture of air or nitrogen with *n*-butane, with *n*-butane/nitrogen and *n*-butane/air ratios equal to 0.015. This *n*-butane/air ratio is similar to that used generally to activate industrial VPO catalysts. The precision of the thermogravimetric analyses was about 2%. $V^{5+}/(V^{5+}+V^{4+})$ ratios for the solids after dehydration were calculated from thermogravimetric analyses on the consideration that the dehydration was total.

### *Other techniques*

The chemical compositions of the solids were determined by atomic absorption. X-ray diffraction analysis was performed on the samples by using a Siemens D 500 diffractometer with $CuK_\alpha$ radiation. $^{31}P$ spin echo spectra were recorded under static conditions on the solids after the thermogravimetric analysis, using a $90°x\text{-}\tau\text{-}180°y\text{-}\tau$ (acquire sequence). The 90° pulse lasted 4.2 μs and τ was 20 μs. For each sample, the irradiation frequency was varied in increments of 100 kHz above and below the $^{31}P$ resonance of $H_3PO_4$. The number of spectra thus recorded was dictated by the frequency limits beyond which no spectral intensity was visible. The $^{31}P$ NMR spin echo mapping information which was obtained by the superposition of all spectra was used for the calibration of the thermogravimetric studies.

## Results

### *Characterization of the precursors*

The physicochemical characteristics of the precursors were published earlier [9]. Chemical analysis showed that the two dopants are present in the precursors with the expected stoichiometry (Table 1). The X-ray diffraction spectra all correspond to $VOHPO_4{\cdot}0.5H_2O$ [6]. The relative (001)/(220) intensities and the BET surface area are slightly modified by doping, which is in agreement with the slight modification of the morphology of the crystallites observed by electron microscopy [10].

### *Thermal and thermogravimetric analyses of the precursors*

The results are presented in Figs 1–5 and Table 2 for the four precursors and the various atmospheres: nitrogen, air, *n*-butane/nitrogen or *n*-butane/air.

In all cases, two ranges of temperature have to be considered. The first, from room temperature up to 330°C, corresponds to the departure of adsorbed species, and the second, from 330°C up to 530°C, to the transformation of the solid. While the first range is approximately always the same, with a mass loss occurring in

**Table 1** Physico-chemical characteristics of the VPO precursors

| Precursors | Co/Co+V | $S_{BET}/m^2\ g^{-1}$ | Adsorbed species/ wt % |
|---|---|---|---|
| VPO | 0 | 11.2 | 2.2 |
| VPOCo1 | 1.05 | 9.1 | 2.6 |
| VPOFe1 | 1.02 | 7.1 | 2.7 |
| VPOCo5 | 5.02 | 6.4 | 3.0 |

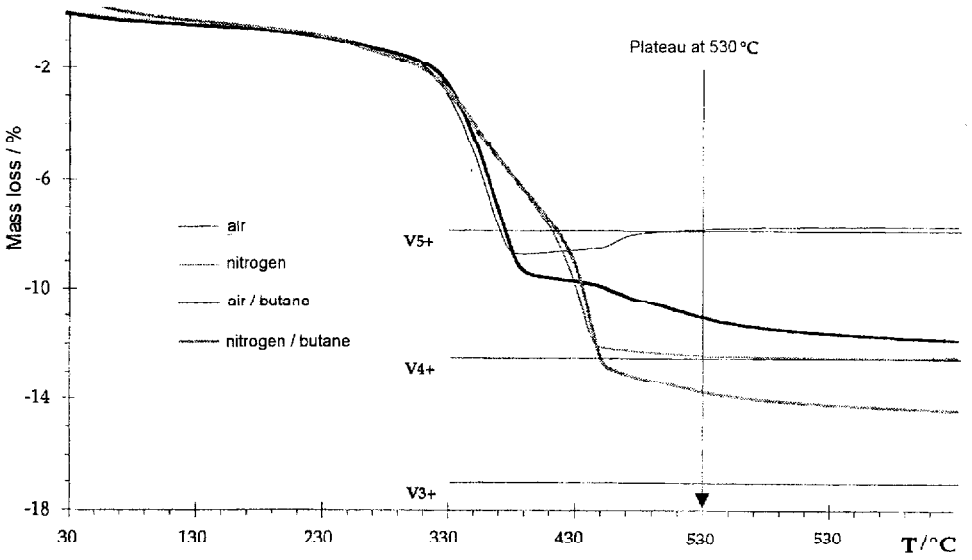


**Fig. 1** TG curves for the VPO precursor under nitrogen, air, nitrogen/butane and air/butane

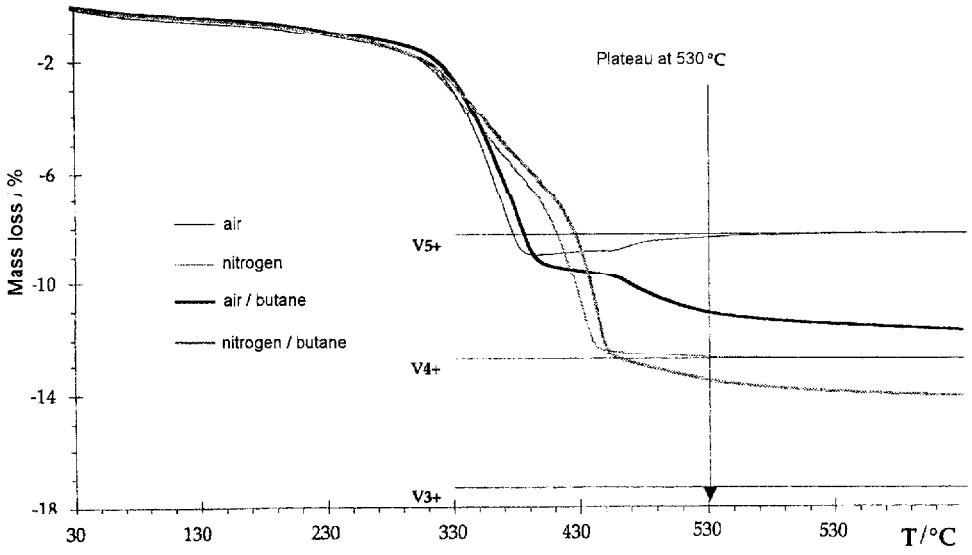


**Fig. 2** TG curves for the VPOCo1 precursor under nitrogen, air, nitrogen/butane and air/butane

two steps at around 60 and 155°C (Fig. 5), the second range differs from one precursor to another and depends strongly upon the atmosphere. The losses which may be attributed to the departure of physisorbed isobutanol and water are re-

**Table 2** Detail of the thermogravimetric analyses of the precursors (Figs 1–4)

| Precursor | Atmosphere | Temperature/°C | | | Final calculated composition/% | | |
|---|---|---|---|---|---|---|---|
| | | a* | b* | c* | $V^{5+}$ | $V^{4+}$ | $V^{3+}$ |
| VPO | nitrogen | 365 | 439 | | 1.8 | 98.2 | – |
| | air | 369* | | 465 | 100 | – | – |
| | nitrogen/*n*-butane | 375 | 446 | | – | 72.5 | 27.5 |
| | air/*n*-butane | | 383 | | 31.1 | 68.9 | – |
| VPOCo1 | nitrogen | 356 | 431 | | 1.1 | 98.9 | – |
| | air | 376** | | 471 | 97.5 | 2.5 | – |
| | nitrogen/*n*-butane | 376 | 446 | | – | 83.0 | 17.0 |
| | air/*n*-butane | | 392 | | 37.2 | 62.8 | – |
| VPOCo5 | nitrogen | 359 | 439 | | 1.8 | 98.2 | – |
| | air | 384** | | 493 | 89.2 | 10.8 | – |
| | nitrogen/*n*-butane | 369 | 451 | | – | 74.5 | 25.5 |
| | air/*n*-butane | | 397 | | 25.0 | 75.0 | – |
| VPOFe1 | nitrogen | 362 | 435 | | 6.8 | 93.2 | – |
| | air | 378* | | 490 | 85.3 | 14.7 | – |
| | nitrogen/*n*-butane | 380 | 443 | | – | 92.6 | 7.4 |
| | air/*n*-butane | | 395 | | 27.3 | 72.7 | – |

* a and b correspond to the losses of hydration and constitutional water respectively; c correspond to the oxidation of the precursors
** transformation corresponding to a and partially to c.

ported in Table 1. It may be seen that they increase with the amount of dopant, whereas at the same time the surface areas of the solids decrease. These results show that the dopants have a great effect on the physisorption of water.

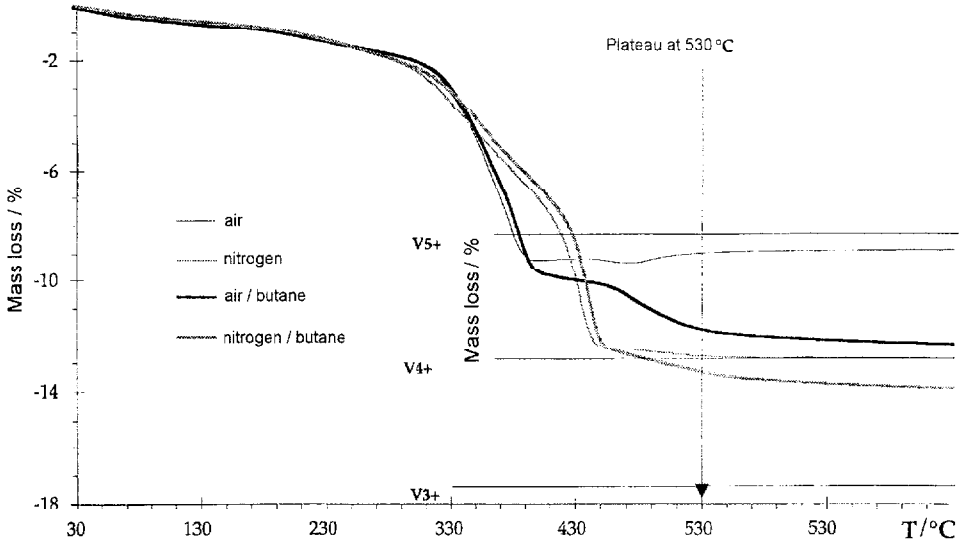


**Fig. 3** TG curves for the VPOFe1 precursor under nitrogen, air, nitrogen/butane and air/butane

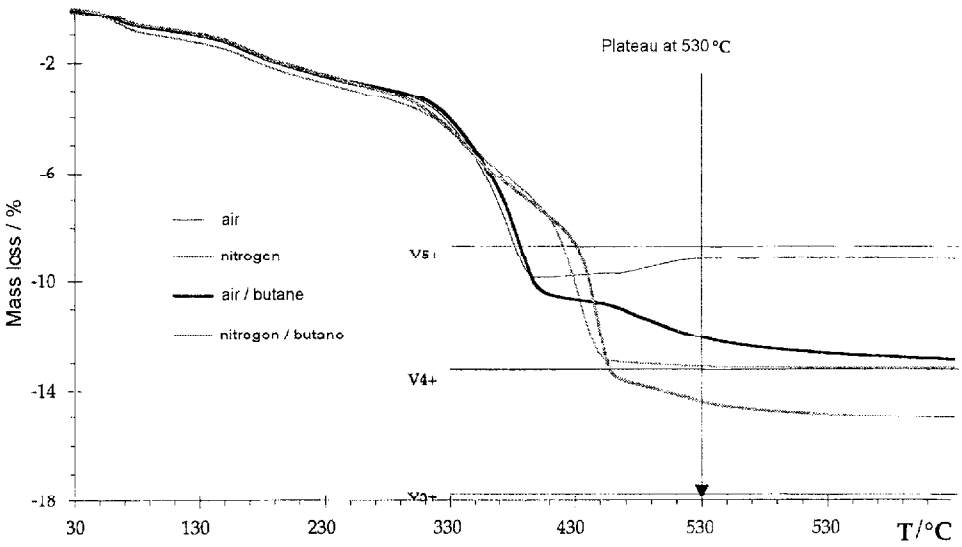


**Fig. 4** TG curves for the VPOCo5 precursor under nitrogen, air, nitrogen/butane and air/butane

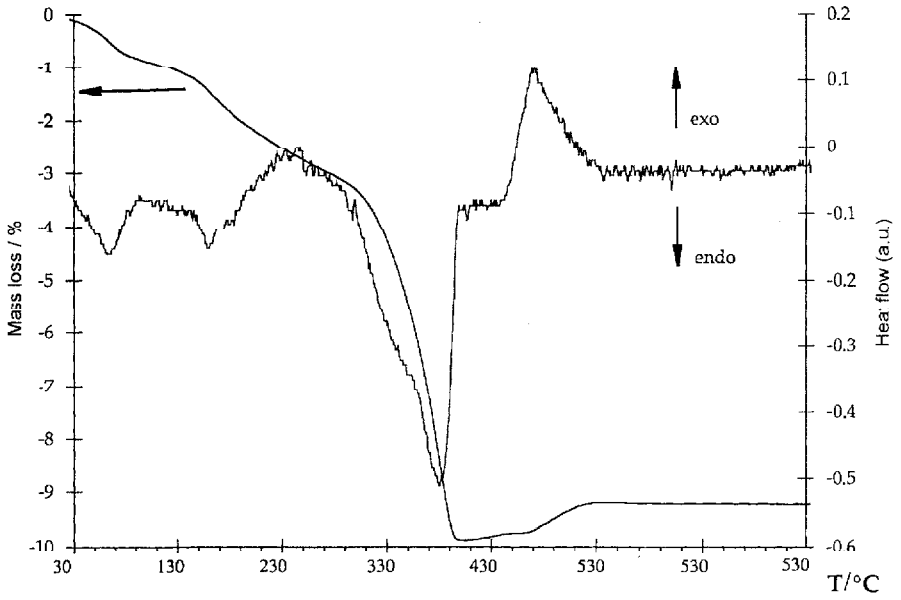


**Fig. 5** Heat flow curve for VPO5 compared with the TG curve for VPO5 under air

## Precursors under nitrogen

The transformation of the undoped VPO precursor under nitrogen (Fig. 1) is similar to that previously described in flowing helium [6]. Two domains can [6] be considered:

1) From room temperature up to 330°C, a continuous loss of mass is observed, which may be attributed to the departure of physisorbed water and isobutanol from the precursor.

2) From 330°C up to 530°C, two mass loss ranges can be considered (330–390°C) and (390–450°C), which correspond successively to the loss of hydration and constitutional water molecules from $VOHPO_4 \cdot 0.5H_2O$. The composition observed at 530°C (Table 2) corresponds to almost quantitative dehydration to $(VO)_2P_2O_7$ (1.8% $V^{5+}$, 98.2% $V^{4+}$).

The transformations of the doped precursors occur at the same temperature as for the undoped precursor and correspond to quantitative dehydration to $(VO)_2P_2O_7$ (Figs 2–4). In this case, doping does not affect the succession of events of the dehydration process:

$$VOHPO_4 \cdot 0.5H_2O \rightarrow VOHPO_4 + 0.5H_2O \quad (a)$$

$$2VOHPO_4 \rightarrow (VO)_2P_2O_7 + H_2O \quad (b)$$

With the exception of VPOFe1 (93.2% $V^{4+}$), the $V^{4+}/V^{5+}$ balances (Table 2) calculated from the compositions at 530°C, after maintenance of the solids for 3 h at this temperature, are all very similar (98.2–98.9% $V^{4+}$), and correspond to the $(VO)_2P_2O_7$ phase detected by X-ray diffraction at the end of the experiment.

### Precursors under air

The thermal behavior of the solids under air is similar for all the precursors, although very different from that under nitrogen. The loss of hydration water (a, b) begins at the same temperature (369°C), but is accelerated and is accompanied by oxidation of the vanadium (c). The two processes which may be concerted can be written

$$VOHPO_4{\cdot}0.5H_2O \rightarrow VOHPO_4+0.5H_2O \quad (a)$$

$$VOHPO_4+0.5O_2 \rightarrow VOPO_4+H_2O \quad (c)$$

At the end of transformation (a), the oxidation is not total and the $V^{5+}/V^{4+}$ balance is the same for VPO and VPOCo1, but lower for VPOCo5 and VPOFe1. The solids remain unchanged up to 460°C, before undergoing oxidation (c). This last transformation, which occurs at 465°C for VPO and at 471°C for VPOCo1, is almost complete in this case (Table 2), while it occurs at 490°C for VPOFe1 and at 493°C for VPOCo5 and is incomplete.

Figure 5 shows the heat flow curve of the VPOCo5 solid, which illustrates transformations (a), (b) and (c) for the successive dehydration (a and b) and oxidation (c) steps.

### Precursors under *n*-butane/nitrogen

The thermal behavior of the solids under butane/nitrogen is similar to that under nitrogen up to 430–450°C. The two dehydration steps (a) and (b) can be identified. The first occurs at the same temperature as under nitrogen, whereas the second occurs 10–15°C higher, depending on the dopant. At 450°C, all the solids are dehydrated and are beginning to undergo a slow and continuous reduction in a range of more than 100°C, according to the process $(VO)_2P_2O_7$+*n*-butane→ $VPO_4$+oxygenated products (d). This reduction is higher for VPO and VPOCo5 than for VPOCo1 and VPOFe1 (Table 2).

### Precursors under *n*-butane/air

The TG curves corresponding to the transformations of the solids under *n*-butane/air and air are similar up to 350–360°C. The same reaction (a) of dehydration may be postulated to take place. However, the oxidation of the solids which occurs as the second transformation is slower than under air and occurs at 383°C for VPO. This temperature increases with the amount of dopant up to 397°C. Af-

ter a stabilization up to 440°C, *n*-butane starts to reduce the oxidized sample. The final $V^{4+}/V^{5+}$ balance measured at 530°C differs, depending on the dopant, and is higher for VPOFe1 and VPOCo5, which demonstrates that Fe has a higher reducing effect than Co (comparable for 1% Fe to 5% Co) (Table 2).

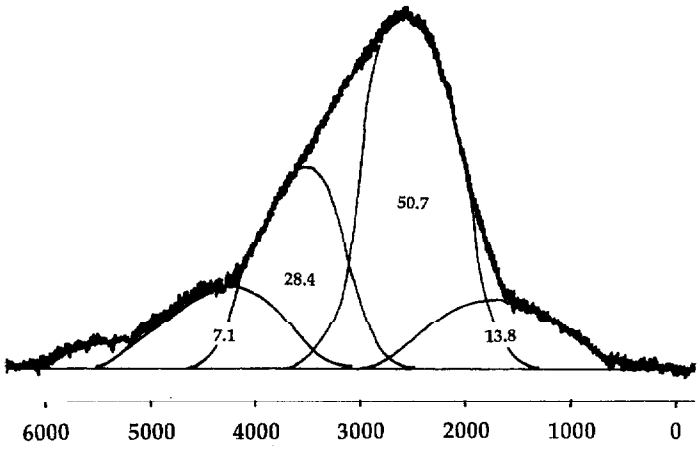


**Fig. 6** $^{31}P$ NMR spectrum by spin echo mapping for VPOCo5 after treatment under nitrogen/butane

The calibration of the oxido-reduction state calculated from the thermogravimetric analysis was confirmed from the $^{31}P$ NMR spectra by spin echo mapping registered for the corresponding solids after thermogravimetric analysis. This is illustrated in Fig. 6 for the case of the VPOCo5 solid after treatment under *n*-butane/nitrogen. The different signals observed can be attributed to structures corresponding to cations $V^{5+}$, $V^{4+}$ and $V^{3+}$ surrounding the phosphorus atoms [8].

i) The signal at 0 ppm corresponds to the $VOPO_4$ structures ($V^{5+}$) (absent in the case of Fig. 6).

ii) The signal in the range 200–1500 ppm corresponds to $V^{4+}$–$V^{5+}$ dimers in a poorly crystallized $(VO)_2P_2O_7$ structure (indexed as $V^{4+}$).

iii) The signal at 2400–2600 ppm (depending on the degree of crystallinity) corresponds to crystallized $(VO)_2P_2O_7$ (indexed as $V^{4+}$).

iv) The signal in the range 3500–5000 ppm (depending on the degree of crystallinity) corresponds to $V^{3+}$ (at 4650 ppm for crystallized $VPO_4$ )[8].

Table 3 shows these main contributions for Fig. 5. The $V^{4+}$ contribution is 13.8% for $V^{4+}$–$V^{5+}$ dimers and 50.7% for crystallized $(VO)_2P_2O_7$, which corresponds to a total of 64.5% indexed as $V^{4+}$, while the $V^{3+}$ contribution is 35.5%. This result is in agreement with the composition of the corresponding solid calculated from the thermogravimetric analysis, which gives 62.5% $V^{4+}$ and 37.5% $V^{3+}$ (Table 2).

**Table 3** Composition of the VPOCo5 solid after thermogravimetric analysis under nitrogen/*n*-butane as measured by $^{31}P$ NMR by spin echo mapping**

| | |
|---|---|
| Signal at 200–1500 ppm (%) | 13.8 |
| Signal at 2400 2600 ppm (%) | 50.7 |
| Signal at 3500–5000 ppm (%) | 35.5 |

**to be compared with Table 2

## Conclusions

The topotactic mechanism of dehydration of $VOHPO_4 \cdot 0.5H_2O$ to $(VO)_2P_2O_7$ in an inert gas flow has been described [6, 11, 12]. The hemihydrate retains its water of hydration up to 350°C. The departure of these molecules results in vacancy formation at the apex of the vanadium-oxygen octahedra. In this stage, an electronic rearrangement proceeds, which corresponds to the formation of $VOHPO_4$ layers. These layers join, expelling the constitutional water molecules to form one $P_2O_7$ group from two $HPO_4$ groups. This second water departure was observed for pure $VOHPO_4 \cdot 0.5H_2O$ at 430°C.

When the hemihydrate is dehydrated in air, the loss of constitutional water takes place at lower temperature (380°C) and partial oxidation of the sample occurs simultaneously, which appears in two steps. Doping with a low percentage (1%) of cobalt delays the temperature of dehydration. This is also observed in *n*-butane/nitrogen and *n*-butane/air mixtures. Doping with cobalt at low percentage also promotes vanadium oxidation. This effect is not observed for doping with iron or a higher percentage of cobalt (5%). This can be explained by a better dispersion of cobalt as compared with that of iron, as evidenced by electron microscopy [10].

The promoting effect of cobalt on the oxidation state of vanadium, which increases the $V^{5+}/V^{4+}$ balance in the *n*-butane/air atmosphere, is highly important to explain the catalytic role of this dopant in *n*-butane oxidation to maleic anhydride, as demonstrated by an *in situ* Raman study [9]. This is made possible by the formation of a very limited solid solution of the type $((VO)_{1-x}Co_x))_2P_2O_7$ [13]. This confirms the specificity of this promoter added in very small amount, as concluded previously by other authors [14].

## References

1 R. A. Varma and D. N. Saraf, Ind. Eng. Chem. Prod. Res. Dev., 18 (1979) 7.
2 B. K. Hodnett, Ph. Permanne and B. Delmon, Appl. Catal., 6 (1983) 231.
3 G. Centi, F. Trifiro, J. R. Ebner and V. M. Franchetti, Chem. Rev., 88 (1988) 55.
4 B. K. Hodnett, Catal. Today, 1 (1987) 477.
5 'Vanadyl Phosphate Catalysts' Catal. Today, Vol. 16, No. 1, G. Centi Ed., Elsevier, Amsterdam 1993.

6 J. W. Johnston, D. C. Johnston, A. J. Jacobson and J. F. Brody, J. Am. Chem. Soc., 106 (1984) 8123.
7 A. Abon, K. E. Bere, A. Tuel and P. Delichère, J. Catal., 156 (1995) 28.
8 M. T. Sananés, A. Tuel and J. C. Volta, J. Catal., 145 (1994) 251.
9 F. Ben Abdelouahab, R. Olier, M. Ziyad and J. C. Volta, J. Catal., 157 (1995) 687.
10 F. Ben Abdelouahab, M. Ziyad, C. Leclercq, J. M. M. Millet, R. Olier and J. C. Volta, J. Chim. Phys., 92 (1995) 1320.
11 E. Bordes, P. Courtine and J. W. Johnston, J. Solid State Chem., 119 (1995) 349.
12 C. C. Torardi, Z. G. Li, H. S. Horowitz, W. Liang and M. H. Whangbo, J. Solid State Chem., 119 (1995) 349.
13 G. J. Hutchings, Appl. Catal., 72 (1991) 1.
14 B. K. Hodnett and B. Delmon, Appl. Catal., 6 (1983) 245.